

Dynamical and photometric imprints of feedback processes on the formation and evolution of E/S0 galaxies.

Michele Cirasuolo¹
 ciras@sissa.it

Francesco Shankar¹
 shankar@sissa.it

Gian Luigi Granato^{2,1}
 granato@pd.astro.it

Gianfranco De Zotti^{2,1}
 dezotti@pd.astro.it
 and

Luigi Danese¹
 danese@sissa.it

ABSTRACT

We show that the observed Velocity Dispersion Function of E/S0 galaxies matches strikingly well the distribution function of virial velocities of massive halos virializing at $z \geq 1.5$, as predicted by the standard hierarchical clustering scenario in a Λ CDM cosmology, for a constant ratio $\sigma/V_{\text{vir}} \simeq 0.55 \pm 0.05$, close to the value expected at virialization if it typically occurred at $z \gtrsim 3$. This strongly suggests that dissipative processes and later merging events had little impact on the matter density profile. Adopting the above σ/V_{vir} ratio, the observed relationships between photometric and dynamical properties which define the fundamental plane of elliptical galaxies, such as the luminosity- σ (Faber-Jackson) and the luminosity-effective radius relations, as well as the $M_{\text{BH}}-\sigma$ relation, are nicely reproduced. Their shapes turn out to be determined by the mutual feedback of star-formation (and supernova explosions) and nuclear activity, along the lines discussed by Granato et al. (2004). To our knowledge, this is the first semi-analytic model for which simultaneous fits of the fundamental plane relations and of the epoch-dependent luminosity function of spheroidal galaxies have been presented.

Subject headings: galaxies: elliptical and lenticular, cD — galaxies: evolution — galaxies: formation — quasars: general

1. INTRODUCTION

¹International School for Advanced Studies, SISSA/ISAS, Via Beirut 2-4, I-34014 Trieste, Italy

²INAF - Osservatorio Astronomico di Padova, Vicolo Osservatorio, I-35100 Padova, Italy

A major challenge for the present day astrophysical research is to trace the evolution of the

Universe from the formation of the first stars in the so called “dark ages” to the present epoch, explaining the variety of structures from galaxies to clusters. Understanding the formation and evolution of spheroidal galaxies, which comprise the most massive and most luminous galaxies in the universe and contain a large fraction of all stars, turned out to be particularly intriguing. Hierarchical models tend to predict substantially fewer massive galaxies at high redshift than are observed (Blain et al. 2002; Scott et al. 2002; Daddi et al. 2003; Tecza et al. 2004; Somerville et al. 2004). On the other hand, the traditional monolithic models, whereby these objects formed their stars on a timescale shorter than their free-fall time and evolved passively thereafter (Eggen, Lynden-Bell & Sandage 1962), do not fit into a coherent scenario for structure formation from primordial density perturbations, and also tend to over-predict high-redshift galaxies.

In this situation it is essential to look for guidance from observational data. It has long been known that stellar populations in elliptical galaxies are old and essentially coeval (Sandage & Visvanathan 1978; Bernardi et al. 1998; Trager et al. 2000; Terlevich & Forbes 2002). A color-magnitude relation is also well established: brighter spheroids are redder (Bower et al. 1992). The widely accepted interpretation is that brighter objects are richer in metals and the spread of their star formation epochs is small enough to avoid smearing of their colors. The slope of this relation does not change with redshift (Ellis et al. 1997; Kodama et al. 1998) supporting this interpretation. The star formation history of spheroidal galaxies is mirrored in the Fundamental Plane (Djorgovski & Davies 1987; Dressler et al. 1987) and in its evolution with redshift. Elliptical galaxies adhere to this plane with a surprisingly low orthogonal scatter ($\sim 15\%$), as expected for a homogeneous family of galaxies. Recent studies (e.g. Treu et al. 2002; van der Wel et al. 2004; Holden et al. 2004, 2005) suggest that ellipticals, both in the field and in clusters, follow this fundamental relation up to $z \sim 1$, consistent with the hypothesis that massive spheroids are old and quiescent.

Direct evidence that massive galaxies with $M \gtrsim 10^{11} M_\odot$ were in place at $z \gtrsim 2$, is provided by recent K -band surveys (Cimatti et al. 2002; Kashikawa et al. 2003; Fontana et al. 2005). The

space density of Extremely Red Objects (EROs) at $z \gtrsim 3$ is only a factor ~ 5 –10 less than at $z \sim 1$ (Tecza et al. 2004).

While the evolution of dark matter halos is controlled only by gravity, and therefore the underlying physics is simple (even if the evolutionary behaviour is complex), processes involving baryons are intricate and may hold the key to reconcile theory with observations. As shown by Granato et al. (2004) the feedback from supernova (SN) explosions and from nuclear activity can reverse the hierarchical scenario for baryons (see also Granato 2001). In other words, the canonical hierarchical Cold Dark Matter (CDM) scheme - small clumps collapse first - is reversed for baryon collapse and the formation of luminous objects (*Anti-hierarchical Baryon Collapse* (ABC) scenario).

In this paper, after a short overview of the Granato et al. (2004) model (Sect. 2), we investigate the imprints of processes governing the formation and the early evolution of spheroidal galaxies on their local dynamic and photometric properties, such as the Velocity Dispersion Function (VDF, Sect. 3.1), the luminosity-velocity dispersion relation (Faber & Jackson 1976, Sect. 3.2), the stellar luminosity-effective radius relation (Bernardi et al. 2003, Sect. 3.3), and the BH mass-velocity dispersion relation (Ferrarese & Merritt 2000; Tremaine et al. 2002; Onken et al. 2004; Sect. 3.4). The main conclusions are presented and discussed in Sect. 4.

Throughout this work we adopt a spatially flat cold dark matter cosmology with cosmological constant, consistent with the Wilkinson Microwave Anisotropy Probe (WMAP) data (Bennett et al. 2003): $\Omega_m = 0.3$, $\Omega_b = 0.047$, and $\Omega_\Lambda = 0.70$, $H_0 = 70 \text{ km s}^{-1} \text{ Mpc}^{-1}$, $\sigma_8 = 0.84$, and an index $n = 1.0$ for the power spectrum of primordial density fluctuations.

2. Overview of the Granato et al. (2004) model

While referring to the Granato et al. (2004) paper for a full account of the model assumptions and their physical justification, we provide here, for the reader’s convenience, a brief summary of its main features.

The model follows with simple, physically grounded recipes and a semi-analytic technique

the evolution of the baryonic component of protospheroidal galaxies within massive dark matter (DM) halos forming at the rate predicted by the standard hierarchical clustering scenario within a Λ CDM cosmology. The main novelty with respect to other semi-analytic models is the central role attributed to the mutual feedback between star formation and growth of a super massive black hole (SMBH) in the galaxy center.

The idea that SN and QSO feedback play an important role in the evolution of spheroidal galaxies has been pointed out by several authors (Dekel & Silk 1986; White & Frenk 1991; Haehnelt, Natarajan & Rees 1998; Silk & Rees 1998; Fabian 1999). Granato et al. (2004) worked out, for the first time, the symbiotic evolution of the host galaxy and the central black-hole (BH), including the feedback. In this model, the formation rate of massive halos ($2.5 \times 10^{11} M_\odot \lesssim M_{\text{vir}} \lesssim 2 \times 10^{13} M_\odot$) is approximated by the positive part of the time derivative of the halo mass function (Press & Schechter 1974, revised by Sheth & Tormen 2002). The gas, heated at virial temperature and moderately clumpy (clumping factor $\simeq 20$), cools to form stars, especially in the innermost regions where the density is the highest. The radiation drag due to starlight acts on the cold gas, further decreasing its angular momentum and causing an inflow into a reservoir around the central BH, to be subsequently accreted into it, increasing its mass and powering the nuclear activity. In turn, the feedbacks from SN explosions and from the active nucleus regulate the star formation rate and the gas inflow, and eventually unbind the residual gas, thus halting both the star formation and the BH growth. In fact, important parameters are the efficiency of SN energy transfer to the cold gas (ϵ_{SN}) and the fraction of the QSO luminosity in winds.

Further relevant differences with other semi-analytic models are the allowance for a clumping factor, $C \simeq 20$, speeding up the radiative cooling so that even in very massive halos ($M_{\text{vir}} \sim 10^{13} M_\odot$), the gas, heated to the virial temperature, can cool on a relatively short (~ 0.5 –1 Gyr) timescale, at least in the dense central regions, and the assumption that the large-scale angular momentum does not effectively slow down the collapse of the gas and the star formation in massive halos virialized at high redshift. As for the latter

assumption, we note that during the fast collapse phase, when the potential well associated with a galactic halo is established, gas clouds can lose their orbital energy to the dark matter by dynamical friction on a timescale shorter than the halo collapse timescale (see, e.g., Mo & Mao 2004).

The model prescriptions are assumed to apply to DM halos virializing at $z_{\text{vir}} \gtrsim 1.5$ and $M_{\text{vir}} \gtrsim 2.5 \times 10^{11} M_\odot$. These cuts are meant to crudely single out galactic halos associated with spheroidal galaxies. Disk (and irregular) galaxies are envisaged as associated primarily to halos virializing at $z_{\text{vir}} \lesssim 1.5$, some of which have incorporated most halos less massive than $2.5 \times 10^{11} M_\odot$ virializing at earlier times, that may become the bulges of late type galaxies. However, the model does not address the formation of disk (and irregular) galaxies and these objects will not be considered in this paper.

The kinetic energy fed by supernovae is increasingly effective, with decreasing halo mass, in slowing down (and eventually halting) both the star formation and the gas accretion onto the central black hole. On the contrary, star formation and black hole growth proceed very effectively in the more massive halos, giving rise to the bright SCUBA phase, until the energy injected by the active nucleus in the surrounding interstellar gas unbinds it, thus halting both the star formation and the black hole growth (and establishing the observed relationship between black hole mass and stellar velocity dispersion or halo mass). Not only the black hole growth is faster in more massive halos, but also the feedback of the active nucleus on the interstellar medium is stronger, to the effect of sweeping out such medium earlier, thus causing a shorter duration of the active star-formation phase.

The basic yields of the model are the star-formation rate, $\psi(t)$, as a function of the galactic age, t , (hence the evolution of the mass in stars, $M_{\text{sph}}(t)$), and the growth of the central BH mass, $M_{\text{BH}}(t)$, for any given value of the halo mass, M_{vir} , and of the virialization redshift, z_{vir} . These quantities are obtained solving the system of differential equations given by Granato et al. (2004), i.e. their eqs. (10), (16), and (23). The rates at which the diffuse gas cools [$\dot{M}_{\text{cold}}(t)$] and forms stars are given by their eqs. (9) and (10), respectively, while

their eq. (16) yields the growth rate – due to the radiation drag mechanism – of the central BH reservoir [$\dot{M}_{\text{inflow}}(t)$], allowing the building-up of the BH mass (eq. 23). Finally, the rates at which the feedback from SN [$\dot{M}_{\text{cold}}^{\text{SN}}(t)$] and QSO [$\dot{M}_{\text{inf}}^{\text{QSO}}$] heats the cold gas moving it into the hot phase are given by their eqs. (11) and (31), respectively. In their notation:

$$\dot{M}_{\text{inf}}(t) = -\dot{M}_{\text{cold}}(t) + \dot{M}_{\text{inf}}^{\text{QSO}} \quad (1)$$

$$M_{\text{gas}}(t) = M_{\text{inf}}(t) + M_{\text{cold,sf}}(t) \quad (2)$$

$$\dot{M}_{\text{res}}(t) = \dot{M}_{\text{inflow}}(t) - \dot{M}_{\text{BH}}(t) \quad (3)$$

$$\begin{aligned} \dot{M}_{\text{cold,sf}}(t) &= \dot{M}_{\text{cold}}(t) - \psi(t) + \dot{M}_{\text{cold}}^{\text{SN}}(t) \\ &\quad + \dot{M}_{\text{cold}}^{\text{QSO}}(t), \end{aligned} \quad (4)$$

where a dot above a symbol denotes a time derivative. Note that, in eq. (10) of Granato et al. (2004), defining $\psi(t)$, $M_{\text{cold}}(r, t)$ is actually $M_{\text{cold,sf}}(r, t)$.

Once the star-formation history, $\psi(t)$, of a galaxy has been computed, its luminosity in any chosen band is obtained, as a function of t , from the GRASIL code (Silva et al. 1998), which, given $\psi(t)$, yields the chemical and the spectro-photometric evolution from the radio to the X-ray band, allowing for the effect of dust absorption and reradiation. GRASIL is available at web.pd.astro.it/granato and at adlibitum.oat.astro.it/silva/default.html. As mentioned above, the halo formation rate is obtained using the Press & Schechter (1974) formalism, as improved by Sheth & Tormen (2002; see eq. (5) of Granato et al. 2004).

Putting these ingredients together we obtain the model predictions for the statistical properties of spheroidal galaxies as a function of cosmic time. Although the model has several parameters (listed in Table 1 of Granato et al. 2004), all of them are strongly constrained by the wealth of observational data that have become available in recent years, including the luminosity functions of spheroidal galaxies at different redshifts, their counts and redshift distributions in optical and near-IR bands, the 850 μm SCUBA counts and the associated (if preliminary) redshift distributions, the relationship between the black-hole mass and the stellar velocity dispersion, the local black-hole mass function, and more (Granato et al. 2004; Silva et al. 2005; Shankar et al. 2004).

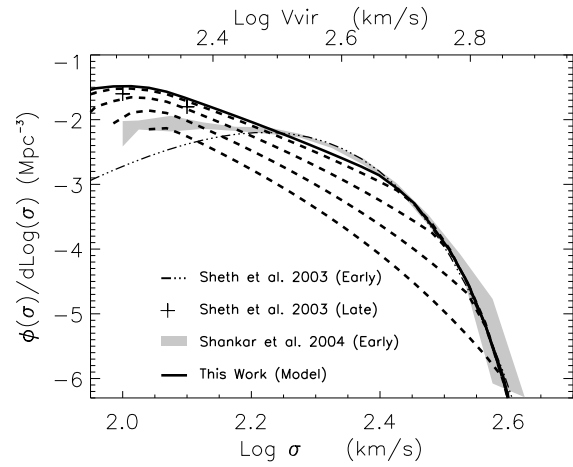


Fig. 1.— Comparison of the virial velocity function of galaxies with $z_{\text{vir}} \geq 1.5$ implied by the standard gravitational clustering scenario (solid line, upper scale), with observational estimates of the velocity dispersion function of early-type galaxies by Shankar et al. (2004; shaded area) and Sheth et al. (2003; triple-dot dashed line). The crosses show the contribution of bulges of late-type galaxies, determined by Sheth et al. (2003). The two functions match for $\sigma = 0.55V_{\text{vir}}$. The dashed lines show the virial velocity functions of galaxies for different choices of the minimum z_{vir} : from top to bottom, $z_{\text{vir,min}} = 2, 3, 4, 5$.

3. Properties of early type galaxies

3.1. The Velocity Dispersion Function

As discussed by Loeb & Peebles (2003), the local Velocity Dispersion Function (VDF) can provide interesting hints on the structure formation process¹. Accurate determinations of the VDF of early-type galaxies have been obtained by Sheth et al. (2003) and Shankar et al. (2004), based on a large sample (~ 9000 E/S0 galaxies) drawn from the SDSS (Bernardi et al. 2003). The two determinations agree remarkably well (see Fig. 1) except for low values of the velocity dispersion, where the Sheth et al. (2003) VDF declines due to the selection criteria adopted by Bernardi et al. (2003) to compute the low luminosity portion of the luminosity function.

As for dark matter halos, it is convenient to

¹Throughout this paper the line-of-sight velocity dispersion σ is referred to $R_e/8$, where the effective radius R_e is defined as the radius containing half of the light.

define a 'virial' velocity, equal to the circular velocity at the virial radius (Navarro et al. 1997, NFW; Bullock et al. 2001):

$$V_{\text{vir}}^2 = \frac{GM_{\text{vir}}}{R_{\text{vir}}}. \quad (5)$$

Since, given the virialization redshift, V_{vir} depends only on M_{vir} ($V_{\text{vir}} \propto M_{\text{vir}}^{1/3}$) the V_{vir} distribution function can be straightforwardly derived from the mass distribution function of spheroidal galaxies [eq. (5) of Granato et al. (2004)], integrated over the virialization redshifts. Following Granato et al. (2004), we assume that all massive halos ($2.5 \times 10^{11} M_{\odot} \lesssim M_{\text{vir}} \lesssim 2 \times 10^{13} M_{\odot}$) virializing at $z \geq 1.5$ yield spheroidal galaxies or bulges of later type galaxies. It may be noted, in passing, that the adopted upper mass limit is close to that inferred by Kochanek & White (2001) from the distribution of gravitational lens image separations.

As illustrated by Fig. 1, the derived V_{vir} distribution function (which depends only on the evolution of dark matter halos) accurately matches the observationally determined VDF (which may be affected by the physics of baryons, and in particular by dissipative processes) if $\sigma \simeq 0.55V_{\text{vir}}$. The best fit and the confidence intervals of the σ/V_{vir} ratio depend somewhat on the choice of the upper mass limit, M_{sup} (reference value $M_{\text{sup}} = 2 \times 10^{13} M_{\odot}$) and of σ_8 (reference value $\sigma_8 = 0.84$), while the choice of the minimum virialization redshift ($z_{\text{vir,min}}$) set at 1.5, does not affect appreciably the fit. For $\sigma_8 = 0.84$, the 95% confidence interval, determined utilizing the χ^2 statistic with 2 degrees of freedom, is $0.53 \leq \sigma/V_{\text{vir}} \leq 0.60$, the upper end corresponding to the smallest value of M_{sup} , which is constrained to be $\geq 10^{13} M_{\odot}$ to ensure consistency with the local K -band luminosity function (see Granato et al. 2004). Decreasing σ_8 to 0.8, yields a 95% confidence interval $0.50 \leq \sigma/V_{\text{vir}} \leq 0.61$, while increasing σ_8 to 0.9, we get an acceptable fit for $M_{\text{sup}} \simeq 10^{13} M_{\odot}$ or $\sigma/V_{\text{vir}} \simeq 0.50$. As already mentioned, the data indicate a σ/V_{vir} ratio independent of virial mass. A weak dependence, not steeper than $\sigma/V_{\text{vir}} \propto M_{\text{vir}}^{0.05}$, is however allowed.

A linear relationship between the central velocity dispersion, σ , and the maximum circular velocity, v_c^{max} – which, for a concentration $c \simeq 3$ (see below), is essentially equal to V_{vir} – was reported

by Gerhard et al. (2001) for a sample of 21 mostly luminous, slowly rotating elliptical galaxies, although the ratio is somewhat higher than found here: $\sigma = 0.66v_c^{\text{max}}$. A weakly non-linear relationship was found by Ferrarese (2002) for a sample of 13 spiral galaxies with rotation curves extending beyond the $B = 25$ mag/arcsec² isophote: $\sigma/200 \text{ km s}^{-1} = 0.60(v_c^{\text{max}}/200 \text{ km s}^{-1})^{1.19}$. According to Ferrarese (2002) this relation can be considered valid also in the σ range populated by elliptical galaxies.

If the stellar velocity dispersion profile is approximately isothermal and stellar velocities are isotropic, adopting the Navarro et al. (1997) density profile we obtain the following relationship between V_{vir} and the velocity dispersion σ :

$$\frac{\sigma}{V_{\text{vir}}} = \frac{\{c[3c^2 + 4c - 2c \ln(1+c) - 2 \ln(1+c)]\}^{1/2}}{\sqrt{6}[1 + (1+c) \ln(1+c)]}, \quad (6)$$

where c , equal to the ratio of R_{vir} to the NFW inner radius r_s , is the "concentration". The N-body simulations by Zhao et al. (2003a) show that halos of mass greater than $10^{11} \text{ h}^{-1} M_{\odot}$ at $z \gtrsim 3$ have all a similar median concentration $c \sim 3.5$. For $c = 2, 3, 4$, eq. (6) yields $\sigma/V_{\text{vir}} = 0.49, 0.57, 0.62$, respectively. Thus, the value of σ/V_{vir} for which we get a match between the local VDF and the V_{vir} distribution function of dark halos is remarkably close to the value expected based on simulations.

The tight correspondence between the VDF and the velocity distribution function of dark halos lends support to the dynamical attractor hypothesis (Loeb & Peebles 2003; Gao et al. 2004), according to which the total distribution of collisionless matter (dark matter plus stars) keeps essentially constant in the presence of merging and of dissipative settling of baryons, with the dark matter distribution expanding to compensate for the dissipative settling of baryons (but see Gnedin et al. 2004 for a different conclusion).

The stability of the stellar dynamics in the central regions of dark halos against merging events subsequent to the virialization redshift is also consistent with the results of detailed numerical simulations (Wechsler et al. 2002; Zhao et al. 2003b) showing that the halo circular velocity changes very little after the end of the initial fast accretion process, during which most of the specific binding energy is assembled, even though a large fraction

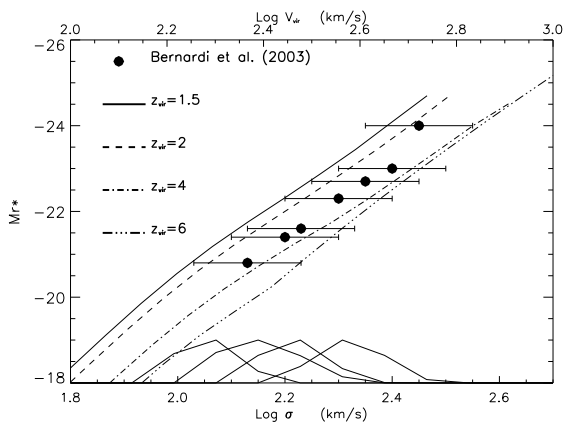


Fig. 2.— Observed Faber-Jackson relation (filled dots) from Bernardi et al. (2003), compared with our predictions for different virialization redshifts z_{vir} . The curves at the bottom of the figure represent the normalized distributions of velocity dispersions of galaxies in 4 absolute magnitude bins 0.5 mag wide, centered at $M_{r^*} = -20.2, -21, -22$, and -23 (from left to right), as predicted by the ABC model. The FWHMs of the predicted distributions are remarkably close to the observed values (FWHM ~ 0.09 ; Bernardi et al. 2003).

of the halo mass is acquired during the subsequent prolonged slow accretion phase.

Figure 1 also shows the contributions to the VDF of different virialization redshifts and highlights that the highest velocity portion comes from the highest virialization redshifts. This result is nicely consistent with the findings by Loeb & Peebles (2003) who computed the expected cumulative comoving VDF at $z = 4$ for the NFW and the Moore et al. (1999) density profile, and found it consistent with the observational determination by Sheth et al. (2003) for velocity dispersions $\sigma > 300 \text{ km s}^{-1}$, while for lower values of σ the predicted VDF is low compared to the observed one. Our curve for $z_{\text{vir}} \geq 4$ has a very similar behavior; but when we allow also for spheroidal galaxies or bulges virializing at lower redshifts we can fully account for the observed VDF. As mentioned above, the contributions of sources virializing at $z \leq 1.5$ is negligibly small.

3.2. The Faber - Jackson relation

Since the first measurements of velocity dispersions of early type galaxies were made, it was recognized that they are correlated with the galaxy luminosities (Poveda 1961; Minkowski 1962). Faber & Jackson (1976) showed that $L_B \propto \sigma^4$ (Faber-Jackson relation). Bernardi et al. (2003), using a sample of ~ 9000 early type galaxies drawn from the Sloan Digital Sky Survey (SDSS) in the redshift range $0.01 \leq z \leq 0.3$, found $L_{r^*} \propto \sigma^{3.92}$, consistent with previous studies (Forbes & Ponman 1999; Pahre et al. 1998). Their data in u , g , i , and z bands show that the relation is roughly independent of wavelength. The distributions of σ at fixed luminosity are approximately Gaussian.

A detailed quantitative analysis can be carried out using the ABC model to follow the time evolution of the baryonic component, both in the gas and in the stellar phase, of each halo mass M_{vir} since the virialization redshift z_{vir} . Then, the present-day luminosity in any chosen band bands from X-ray to radio can be computed with the spectrophotometric code GRASIL (Silva et al. 1998) as a function of V_{vir} , which is uniquely determined by the value of M_{vir} , given z_{vir} . As illustrated by Fig. 2, the model not only predicts the correct slope of the Faber-Jackson relation, but also the correct normalization, when we use the ratio $\sigma/V_{\text{vir}} = 0.55$ found from the analysis of the VDF. Acceptable fits can be obtained with $0.50 \lesssim \sigma/V_{\text{vir}} \lesssim 0.65$ (again, the confidence interval is derived using the χ^2 statistic).

The scatter in the observed relation is interpreted as an intrinsic property of elliptical galaxies, accounted for by different virialization epochs: galaxies with the same spheroidal luminosity, but virializing at lower redshifts, have lower velocity dispersions. The curves at the bottom of Fig. 2 show the σ distributions (arbitrary units) of galaxies in four luminosity bins, as obtained from the Granato et al. (2004) model. Such distributions have been computed integrating over cosmic time, for each value of σ , the formation rate of halos with present day luminosities within the considered bin; they turn out to be roughly Gaussian, with the peak close to the σ expected from the best fit relation and FWHM in agreement with that observed by Bernardi et al. (2003).

It is worth noting that the standard scaling of

the virial parameters in the hierarchical clustering scenario gives (Bullock et al. 2001) $M_{\text{vir}} \propto V_{\text{vir}}^3 (1 + z_{\text{vir}})^{-3/2}$, which, for a roughly constant M_{vir}/L ratio, would imply a flatter slope than is observed in the Faber-Jackson relation. However, the slope is steepened in the ABC model which predicts a decrease of the $M_{\text{vir}}/M_{\text{sph}}$ ratio (M_{sph} being the mass in stars), with increasing M_{vir} , whose details depend on the virialization redshift (see Fig. 5 of Granato et al. 2004). This is due to feedback from supernovae, which is increasingly efficient with decreasing M_{vir} in preventing the gas from cooling and forming stars, tempered by the feedback from active nuclei which is more effective in the more massive objects. On average, we have, to a sufficient approximation, $M_{\text{vir}}/M_{\text{sph}} \propto M_{\text{vir}}^{-1/5}$. The ABC model also predicts an essentially constant M_{sph}/L ratio (the observed weak luminosity dependence is attributed to the systematic changes with luminosity of the galactic structure, see Sect. 3.3). Therefore, the $M_{\text{vir}}-V_{\text{vir}}$ relation, for $\sigma/V_{\text{vir}} = \text{const}$, translates into $L \propto \sigma^{18/5} (1 + z_{\text{vir}})^{-9/4}$. The mean slope steepens somewhat, approaching that of the observed Faber-Jackson relation, when we account for the varying contributions of different virialization redshifts to different σ intervals. A further steepening of the Faber-Jackson relation is expected at low σ values, corresponding to less massive objects where the SN feedback, yielding $M_{\text{vir}}/M_{\text{sph}} \propto M_{\text{vir}}^{-1/2}$, dominates.

In conclusion, the Faber-Jackson relation is interpreted as providing a quantitative measure of the effect of feedback, and primarily of the effect of the energy injected onto the interstellar medium by supernovae. The close agreement with the predictions of the ABC confirms the correctness of the adopted recipes. We note that fitting simultaneously the galaxy epoch dependent luminosity functions and dynamical properties has long been a very challenging problem for semi-analytic models (see, e.g., Mo & Mao 2004). In the case of spheroidal galaxies, this requires that the model correctly predicts not only the evolution of L/M_{vir} but also the distribution of virialization redshifts as a function of the present-day luminosity. To our knowledge, this is the first semi-analytic model for which successful fits of all these quantities have been reported.

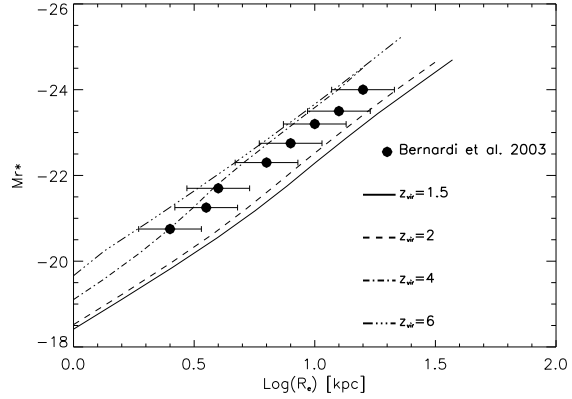


Fig. 3.— Absolute magnitude in the r^* band versus R_e . The data points are from Bernardi et al. (2003) while the lines show our model predictions for different virialization redshifts.

3.3. Completing the Fundamental Plane

An additional, though not independent, check on the physical processes involving baryons in the ABC model is provided by the observed $L-R_e$ relation (see e.g. Bernardi et al. 2003). The effective radius, like the velocity dispersion, is related to the collapse and settling of the baryonic component inside the DM potential well. On the other hand, the model does not give us dynamical information. However, it yields the total mass in stars and dark remnants, while observations ensure that the starlight distribution in spheroids has quite a uniform shape. In fact the surface brightness distribution is well represented by $\log(I(r)) \propto r^{1/n}$ (Sersic 1968); the classical de Vaucouleurs profile has $n = 4$ (de Vaucouleurs 1948).

Borriello et al. (2003), properly taking into account the light distribution, the mass traced by light, and the dark matter, found that the effective radius can be written as:

$$R_e = (k_\sigma + \alpha_{\text{DM}}) \frac{GM_{\text{sph}}}{\sigma^2}, \quad (7)$$

where M_{sph} is the total mass traced by light, k_σ is a constant depending on the light distribution ($k_\sigma = 0.174$ for the de Vaucouleurs profile) and α_{DM} is a function of the DM mass inside R_e and of its density distribution [see eqs. (13) and (14) of Borriello et al. 2003]. As found by Gerhard et al. (2001) for a sample of about 20 elliptical galaxies and generalized by Borriello et al. (2003) on the

basis of the narrowness of the Fundamental Plane, the DM inside the effective radius amounts to only 10-50% of the total mass. Such an amount and its distribution make α_{DM} almost negligible in the above equation, that can be rearranged as follows, using the definition of V_{vir} [eq. (5)]:

$$\frac{R_e}{R_{\text{vir}}} = (k_\sigma + \alpha_{\text{DM}}) \frac{M_{\text{sph}}/M_{\text{vir}}}{(\sigma/V_{\text{vir}})^2}, \quad (8)$$

The ABC model yields the $M_{\text{sph}}/M_{\text{vir}}$ ratio and the ensuing M_{sph}/L ratio, whose value depends on the adopted IMF. Using the Salpeter's IMF we get $M_{\text{sph}}/L_r \simeq 5 M_\odot/L_\odot$, with very little dependence on the luminosity in the reference r^* band.

On the other hand, systematic changes with luminosity of the galactic structure, quantified by the Sersic index n , have been reported and found to account for the variation of the M/L ratio with luminosity (Ciotti et al 1996; Graham et al. 2001; Trujillo et al. 2004). Bernardi et al. (2003), exploiting the large sample of early-type galaxies in the SDSS, defined an effective mass $M_0 \equiv 4R_e\sigma^2/G$, and found $M_0/L_r = 3.5(L_r/L_r^*)^{0.15}$, in solar units, with $L_r^* = 2 \times 10^{10} L_\odot$. After eq. (7) $M_0 = 4(k_\sigma + \alpha_{\text{DM}})M_{\text{sph}}$, so that, neglecting α_{DM} and setting $M_{\text{sph}}/L_r \simeq 5 M_\odot/L_\odot$, we have:

$$k_\sigma \simeq 0.174 \left(\frac{L_r}{L_r^*} \right)^{0.15}, \quad (9)$$

consistent with the findings of Borriello et al. (2003) based on a much smaller sample (221 nearby galaxies) but with more detailed observations. Hence:

$$\frac{R_e}{R_{\text{vir}}} \simeq 0.87 \left(\frac{L_r}{L_r^*} \right)^{0.15} \frac{L_r/M_{\text{vir}}}{(\sigma/V_{\text{vir}})^2}. \quad (10)$$

The ABC model gives, for each value of z_{vir} and for an assumed IMF, R_{vir} and L_r as a function of M_{vir} . Using the above equation we can then obtain a relationship between L_r (or the absolute magnitude M_{r^*}) and R_e . The results for a Salpeter IMF and $\sigma/V_{\text{vir}} = 0.55$, as implied by the VDF, are compared in Fig. 3 with the data of Bernardi et al. (2003). The presence of an average $\sim 30\%$ of DM inside R_e would imply $\alpha_{\text{DM}} \leq 0.02$ (see Borriello et al. 2003) and would not modify the fit.

The $M_{r^*}-R_e$ relation is related to the Faber-Jackson relation through eq. (7), given the observationally determined L_r/M_{sph} ratio. Thus,

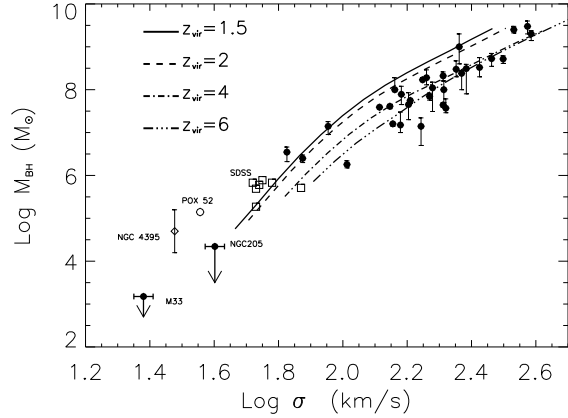


Fig. 4.— The $M_{\text{BH}} - \sigma$ relation predicted by the model for different virialization redshifts compared with observational data. Filled circles represent nearby galaxies with dynamical measurements of the BH mass (Tremaine et al. 2002) and the upper limits for M33 (Gebhardt et al. 2001) and NGC 205 (Valluri et al. 2005). Open symbols refer to galaxies with BH masses estimated from the $H\beta$ linewidth-luminosity-mass relation: NGC 4395 (open diamond; Filippenko & Ho 2003), POX 52 (open circle; Barth et al. 2004) and a sample of 7 faint active nuclei drawn from the SDSS, (open squares; Greene et al. 2004).

it does not provide an independent test of the L_r/M_{vir} ratio predicted by the ABC model. Still, the consistency of the model with a different set of data is, at least, reassuring.

3.4. The central black hole

In the last years massive BHs were proven to be ubiquitous in massive E/S0 galaxies (see e.g. Magorrian et al. 1998). Tight relations have been discovered between BH masses, M_{BH} , and stellar velocity dispersions (Ferrarese & Merritt 2000; Gebhardt et al. 2000; Tremaine et al. 2002; Onken et al. 2004), masses of the spheroidal components (McLure & Dunlop 2002; Dunlop et al. 2003; Marconi & Hunt 2003), and masses of the dark halos (Ferrarese 2002); see Ferrarese & Ford (2004) for a comprehensive review. The $M_{\text{BH}}-\sigma$ relationship has been extensively discussed as a probe of the interplay between QSO and host galaxy evolution (Silk & Rees 1998; Fabian 1999; Cavaliere et al. 2002).

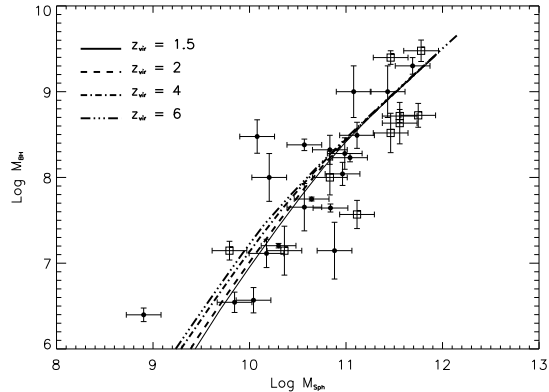


Fig. 5.— Predicted M_{BH} – M_{sph} relation for different virialization redshifts compared with observational data from Häring & Rix (2004). Open squares are sources from their Group 1 and solid circles from their Group 2.

Granato et al. (2004) showed that the growth of the stellar component and of the central BH are strictly symbiotic, double tied by the positive effect of the photon drag, proportional to the star formation rate, favoring the inflow toward the reservoir around the central BH (Umemura 2001; Kawakatu & Umemura 2002), and by the negative effect of the BH growth, powering outflows.

The ABC model follows, for any given M_{vir} and z_{vir} , the growth of the central BH and gives its final mass. The predicted $M_{\text{BH}}-V_{\text{vir}}$ relation, at fixed z_{vir} , is immediately translated into $M_{\text{BH}}-\sigma$ using the ratio $\sigma/V_{\text{vir}} = 0.55$ derived from the VDF. The scatter of data points is interpreted as reflecting the distribution of z_{vir} .

The model also predicts a steepening of the relation at low σ values, due to the combined effect of SN feedback – which is increasingly efficient with decreasing halo mass in slowing down the gas infall onto the central BH – and of the decreased radiation drag (due to a decrease of the optical depth). From an observational point of view, the behavior of the $M_{\text{BH}}-\sigma$ relation in the low BH mass and low velocity dispersion regime is still unclear, due to the dearth of data and to the uncertainties on the M_{BH} estimates. In Fig. 4 we plot objects found in literature with estimated BH masses $M_{\text{BH}} \lesssim 10^6 M_{\odot}$. Dynamical measurements are available only for M33 and

NGC 205, while all the other BH masses have been estimated through the linewidth-luminosity-mass scaling relation (Kaspi et al. 2000). Therefore the cases of M33 and NGC 205 are particularly interesting, although they are outside the range of masses to which we applied our model up to now. For M33 the upper limit to the BH mass is $M_{\text{BH}} \lesssim 3000 M_{\odot}$ (Merritt et al. 2001) or $M_{\text{BH}} \lesssim 1500 M_{\odot}$ (Gebhardt et al. 2001), while, for NGC 205, $M_{\text{BH}} \lesssim 2.2 \times 10^4 M_{\odot}$. Both fall below the extrapolation of the $M_{\text{BH}}-\sigma$ relation holding at higher σ (Ferrarese & Merritt 2000; Gebhardt et al. 2000; Tremaine et al. 2002; Onken et al. 2004), while it is fully consistent with the extrapolation of our model. On the other hand, the BH mass estimates for the faint type 1 Seyfert nuclei in NGC 4395 (Filippenko & Ho 2003), in POX 52 (Barth et al. 2004) and in 7 galaxies drawn from SDSS (Greene et al. 2004) are only marginally consistent with the steepening predicted by our model. More data on the so called intermediate mass BHs ($10^3 M_{\odot} \lesssim M_{\text{BH}} \lesssim 10^6 M_{\odot}$) in the galactic centers (see van der Marel (2003) for a review) are needed to clarify this issue. Of course we should also keep in mind that the low BH mass portion of the diagram might just reflect the distribution of BH seeds (possibly created by merging of smaller BHs during the fast accretion epoch) and be only weakly affected by the mass accretion which is controlled by the effects discussed above. For example, Koushiappas et al. (2004) presented a model yielding seed BHs with characteristic masses $\sim 10^5 M_{\odot}$. Also, low BH masses may be easily increased by substantial factors during later accretion phases, when host galaxies are disk- (rather than bulge-) dominated.

Another prediction of the ABC model is that the ratio of the BH mass to the mass in stars, $M_{\text{BH}}/M_{\text{sph}}$, is almost insensitive to variations of z_{vir} . Therefore the $M_{\text{BH}}-M_{\text{sph}}$ relation is expected to have a smaller *intrinsic* scatter (see Fig. 5) than the $M_{\text{BH}}-\sigma$ relation. This is because, as mentioned above, the growth of the BH mass is controlled by the star formation rate through the radiation drag and the SN feedback, and in turn, the feedback from the active nucleus can eventually sweep out the gas thus halting both the star formation and the accretion on the BH. Thus the stellar and BH mass grow (and stop growing) in parallel. The parallelism is not exact, however,

since the star formation rate has a twofold effect on the BH growth. As a result, the $M_{\text{BH}}-M_{\text{sph}}$ relation is not strictly linear, but bends down at small masses, and is slightly different for different values of z_{vir} . On the other hand, estimates of M_{sph} are somewhat indirect and therefore liable to larger uncertainties than those of σ , that can be directly measured; this may translate in an *observed* scatter around the mean $M_{\text{BH}}-M_{\text{sph}}$ relation comparable to, or larger than that for the $M_{\text{BH}}-\sigma$ relation, in spite of the smaller intrinsic scatter.

In Fig. 5 we plot the $M_{\text{BH}}-M_{\text{sph}}$ relation for objects with reliable bulge mass determinations from Häring & Rix (2004). The agreement between the data, suggesting a slightly non-linear relation ($M_{\text{BH}} \propto M_{\text{sph}}^{1.12}$), with our predictions is remarkably good. As pointed out by Häring & Rix (2004), a significant fraction of the scatter (which is $\lesssim 0.3$ dex) can be attributed to measurement errors. Marconi & Hunt (2003) found that the scatter in this relation is reduced to ~ 0.25 dex, when M_{sph} is estimated as a virial mass ($\sim R_e \sigma^2$).

The very good fits of the observed $M_{\text{BH}}-\sigma$ and $M_{\text{BH}}-M_{\text{sph}}$ relations are additional strong indications that the ABC model properly includes the mutual feedbacks of stars and QSOs. It is worth noticing that the model also correctly predicts the local BH mass function in spheroidal galaxies (Granato et al. 2004; Shankar et al. 2004).

4. Discussion and conclusions

We have pointed out an impressively, and unexpectedly, tight correspondence between the virial velocities, V_{vir} , controlled by the dynamics of dark halos, and the stellar velocity dispersions, σ , that feel the effect of dissipative baryon loading. A straightforward comparison of the virial velocity distribution, implied by the standard hierarchical clustering scenario in a Λ CDM cosmology, with the observed velocity dispersion function of spheroidal galaxies, shows that the two functions match remarkably well for a constant ratio $\sigma/V_{\text{vir}} \simeq 0.55$. For a NFW density profile, this ratio corresponds to a concentration parameter $c \simeq 3$, noticeably close to that found from N-body simulations (Zhao et al. 2003a) to apply to halos of mass greater than $10^{11} \text{ h}^{-1} M_\odot$ virializing at $z \gtrsim 3$, with no significant dependence

on halo mass. Thus the matter density profile at virialization appears to be essentially unaffected by the subsequent events, including mergers and the dissipative contraction of baryons, consistent with the dynamical attractor hypothesis (Loeb & Peebles 2003; Gao et al. 2004).

The $V_{\text{vir}}-\sigma$ relation is a key ingredient to connect theoretical predictions with observations. Using the above determination of the σ/V_{vir} ratio, we have shown that the observed relationships between photometric and dynamical properties of spheroidal galaxies, defining the Fundamental Plane, carry clear imprints of the feedback processes ruling the early evolution of spheroidal galaxies. The steeper slope of the luminosity- σ (Faber-Jackson) relation compared to the predicted $M_{\text{vir}}-V_{\text{vir}}$ relation is interpreted as due primarily to the heating of the interstellar medium by supernovae, which increasingly hampers star-formation in smaller and smaller halos, and to winds driven by the active nucleus, that eventually sweep out the residual interstellar gas in the most massive nuclei. A full analysis shows that the treatment of feedback adopted in the ABC model nicely accounts not only for the slope, but also for the normalization of the Faber-Jackson relation (see Fig. 2). The model implies that the observed scatter is mostly intrinsic and due to the spread of virialization redshifts. It also predicts a moderate steepening of the relation at low masses. To our knowledge, this is the first semi-analytic model for which simultaneous fits of the epoch dependent luminosity functions and of the Faber-Jackson relation have been reported.

The effect of feedback also determines the slope of the luminosity-effective radius relation. As discussed in Sect. 3.2, the feedback yields, approximately, $M_{\text{vir}} \propto M_{\text{sph}}^{5/6}$. Then, taking into account eq. (8), neglecting α_{DM} and with $k_\sigma \propto L_r^{0.15}$, we get, from $M_{\text{vir}} \propto R_{\text{vir}}^3$ (for given z_{vir}), $R_e \propto L_r^{0.15} R_{\text{vir}}^{8/5}$ and $L_r \propto R_e^2$. Weighting with the redshift distributions appropriate for each value of R_e (high- z galaxies contribute more to low R_e 's), the mean L_r-R_e relationship flattens towards the observed relation $L_r \propto R_e^{1.58}$ (Bernardi et al. 2003). A further flattening is predicted at low R_e values, where the SN feedback dominates, yielding, approximately, $M_{\text{vir}} \propto M_{\text{sph}}^{2/3}$, whence $R_e \propto L_r^{0.15} R_{\text{vir}}^{5/2}$ and $L_r \propto R_e^{1.4}$. Again, the model

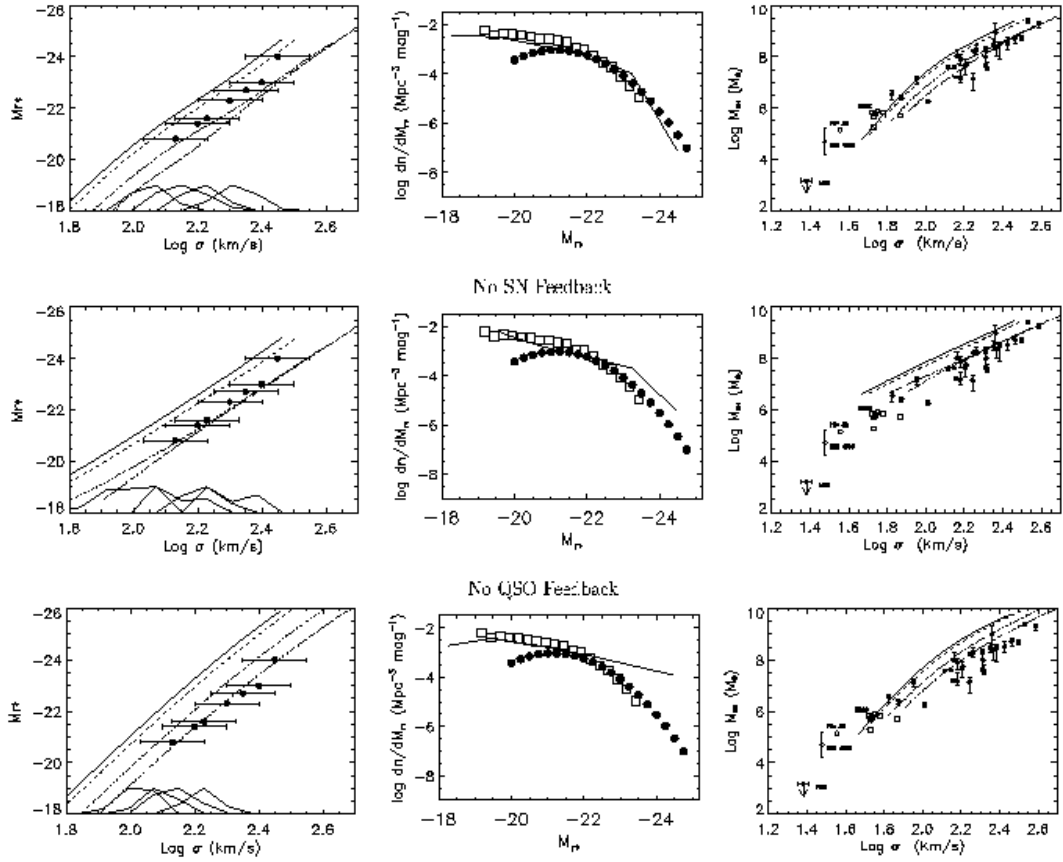


Fig. 6.—Effect of feedback on the Faber-Jackson relation (left panel column), on the local r^* -band luminosity function of spheroidal galaxies (central panel column), and on the $M_{\text{BH}}-\sigma$ relation (right panel column), according to the ABC model. The upper, central, and lower panel rows compare with the data the ABC model predictions with feedback fully included and switching off, in turn, the SN and the QSO feedback, respectively. Symbols are as in Figs. 2 and 4. The observational determinations of the local luminosity function are from Nakamura et al. (2002; open squares), and Bernardi et al. (2003; filled circles).

correctly reproduces not only the slope but also the normalization of the relation (see Fig. 3). As in the case of the Faber-Jackson relation, we expect a scatter comparable to the observed one due to the different virialization redshifts. Although the L_r-R_e and the Faber-Jackson relation do not provide independent tests of the model (see Sect. 3.3) it is reassuring that two different data sets consistently confirm that it yields the correct virial mass-to-light ratio.

The evolution of the stellar component is tied to that of the central black hole, and therefore the $M_{\text{BH}}-\sigma$ relation is also shaped by the effect of feedback, primarily from the active nucleus itself

in the more massive systems, and from supernovae in smaller objects. Again, observations are well reproduced (see Fig. 4), the dispersion around the best-fit relation is expected to be largely due to the different virialization redshifts, and a steepening of the $M_{\text{BH}}-\sigma$ is expected for low BH masses, if these are mostly due to accretion interrelated with the bulge formation. However, small BH masses may be substantially increased by later accretion, occurring when the host galaxy is disk-dominated. Moreover, according to some analyses, seed BH masses may be $\sim 10^5 M_{\odot}$, and the low- σ portion of the diagram is testing more the distribution of seed masses than the accretion history.

We have further pointed out that the $M_{\text{BH}}-M_{\text{sph}}$ relationship is essentially independent of z_{vir} (see Fig. 5); its *intrinsic* scatter should therefore be minimum, although this does not necessarily translate in a low *observed* scatter due to the large uncertainties on the M_{sph} estimates (compared to those on σ).

A synoptic view of the effect of feedback on the luminosity- σ relation, on the local r^* -band luminosity function, and on the $M_{\text{BH}}-\sigma$ relation, based on the ABC model, is provided by Fig. 6. If we switch off the supernova feedback (central panel row), we get a larger luminosity at fixed virial velocity V_{vir} . The increase is of $\simeq 1$ mag. for low luminosity/mass galaxies ($M_{r^*} \simeq -20$), where the stellar feedback is dominating over the QSO feedback, and of 0.5 mag. at high luminosities ($M_{r^*} \simeq -23$). Turning off the QSO feedback (bottom panel row) goes in the same direction, but now the effect is larger for larger galaxies. To fit the observed Faber-Jackson relation with no stellar or QSO feedback, we have to shift by 0.1 dex the σ/V_{vir} ratio, but this is inconsistent with the observed VDF.

As shown by the central panel column of Fig. 6, the shift to higher luminosities occurring when the feedback is switched off affects only weakly the low luminosity portion of the luminosity function, because of its flat slope. On the other hand, the high luminosity tail is very sensitive to it, and particularly to the feedback from the active nuclei.

On the whole, the local luminosity function of galaxy spheroids and the observed correlations between their properties provide clear evidence that the feedback both from supernovae and from active nuclei plays a key role in the evolution of these sources, and yield rather stringent constraints on the parameters controlling the coupling of the energy injected into the interstellar medium.

5. Acknowledgments

We are grateful to the referee for useful comments. Financial support from the Italian MIUR and INAF is acknowledged.

REFERENCES

Barth, A.J., Ho, L.C., Rutledge, R.E., & Sargent, W.L.W. 2004, ApJ, 607, 90

Bennett, C.L., et al. 2003, ApJ, 583, 1

Bernardi, M., et al. 1998, ApJ, 508, 143

Bernardi, M., et al. 2003, AJ, 125, 1849

Blain, A.W., Smail, I., Ivison, R.J., Kneib, J.-P., & Frayer, D.T. 2002, PhR, 369, 111

Borriello, A., Salucci, P., & Danese L. 2003, MNRAS, 341, 1109

Bower, R.G., Lucey, J.R., & Ellis R.S. 1992, MNRAS, 254, 601

Bullock, J.S., Kolatt, T.S., Sigad, Y., Somerville, R.S., Kravtsov, A.V., Klypin, A.A., Primack, J.R., & Dekel, A. 2001, MNRAS, 321, 559

Cavaliere, A., Lapi, A., & Menci, N. 2002, ApJ, 581, L1

Cimatti, A., et al. 2002, A&A, 391, L1

Ciotti, L., Lanzoni, B., & Renzini, A. 1996, MNRAS, 282, 1

Daddi, E., et al. 2003, ApJ, 588, 50

Dekel, A., & Silk, J. 1986, ApJ, 303, 39

de Vaucouleurs, G. 1948, Ann. d'Astroph., 11, 247

Djorgovski, S.G., & Davis, M. 1987, ApJ, 313, 59

Dressler, A., Lynden-Bell, D., Burstein, D., Davies, R.L., Faber, S.M., Terlevich, R., & Wegner, G. 1987, ApJ, 313, 42

Dunlop, J.S., McLure, R.J., Kukula, M.J., Baum, S.A., O'Dea, C.P., & Hughes, D.H. 2003, MNRAS, 340, 1095

Eggen, O.J., Lynden-Bell, D., & Sandage, A. 1962, ApJ, 136, 748

Ellis, R.S., Smail, I., Dressler, A., Couch, W.J., Oemler, A., Butcher, H., & Sharples, R.M. 1997, ApJ, 483, 582

Faber, S.M., & Jackson, R. E. 1976, ApJ, 204, 668

Fabian, A.C. 1999, MNRAS, 308, L39

Ferrarese, L., & Merritt, D. 2000, ApJ, 539, L9

Ferrarese, L. 2002, ApJ, 578, 90

Ferrarese, L., & Ford, H. 2004, astro-ph/0411247

Filippenko, A.V., & Ho, L.C. 2003, ApJL, 588, L13

Fontana, A., et al. 2005, A&A, in press, (astro-ph/0405055)

Forbes, D.A., & Ponman, T.J. 1999, MNRAS, 309, 623

Gao, L., Loeb, A., Peebles, P.J.E., White, S.D.M., & Jenkins, A. 2004, ApJ, 614, 17

Gebhardt, K., et al. 2000, ApJ, 539, L13

Gebhardt, K., et al. 2001, AJ, 122, 2469

Gerhard, O., Kronawitter, A., Saglia, R.P., & Bender, R. 2001, AJ, 121, 1936

Gnedin, O.Y., Kravtsov, A.V., Klypin, A.A., & Nagai, D. 2004, ApJ, 616, 16

Granato, G.L., De Zotti, G., Silva, L., Bressan, A., & Danese, L. 2004, ApJ, 600, 580

Granato, G.L., Silva, L., Monaco, P., Panuzzo, P., Salucci, P., De Zotti, G., & Danese, L. 2001, MNRAS, 324, 757

Graham, A.W., Trujillo, I., & Caon, N. 2001, AJ, 122, 1707

Greene, J.E., Ho, L.C., & Barth, A.J. 2004, in IAU Symp. 222, (astro-ph/0406047)

Haehnelt, M.G., Natarajan, P., & Rees, M.J. 1998, MNRAS, 300, 817

Häring, N., & Rix, H.-W. 2004, ApJ, 604, 89

Holden, B.P., van der Wel, A., Franx, M., et al. 2005, ApJ, 620, L83

Holden, B.P., Stanford, S.A., Eisenhardt, P., & Dickinson, M. 2004, AJ, 127, 2484

Kashikawa, N., et al. 2003, AJ, 125, 53

Kaspi, S., Smith, P.S., Netzer, H., Maoz, D., Jannuzi, B.T., & Giveon, U. 2000, ApJ, 533, 631

Kawakatu, N., & Umemura, M. 2002, MNRAS, 329, 572

Kochanek, C.S., & White, M. 2001, ApJ, 559, 531

Kodama, T., Arimoto, N., Barger, A.J., & Aragón-Salamanca, A. 1998, AA, 334, 99

Koushiappas, S.M., Bullock, J.S., & Dekel, A. 2004, MNRAS, 354, 292

Loeb, A., & Peebles, P.J.E. 2003, ApJ, 589, 29

Marconi, A., & Hunt, L. 2003, ApJL, 589, L21

McLure, R.J. & Dunlop, J.S. 2002, MNRAS, 331, 795

Merritt, D., Ferrarese, L., & Joseph, C.L. 2001, Science, 293, 1116

Minkowski, R. 1962, in IAU Symposium 15, Problems of Extra-Galactic Research, . Ed. G.C. McVittie, 112

Mo, H.J., & Mao, S. 2004, MNRAS, 353, 829

Moore, B., Ghigna, S., Governato, F., Lake, G., Quinn, T., Stadel, J., & Tozzi, P. 1999, ApJ, 524, L19

Nakamura, O., Fukugita, M., Yasuda, N., Loveday, J., Brinkmann, J., Schneider, D.P., Shimasaku, K., & SubbaRao, M. 2003, AJ, 125, 1682

Navarro, J.F., Frenk, C.S., & White, S.D.M. 1997, ApJ, 490, 493

Onken, C.A., Ferrarese, L., Merritt, D., Peterson, B.M., Pogge, R.W., Vestergaard, M., & Wandel, A. 2004, ApJ, 615, 645

Pahre, M.A., Djorgovski, S.G., & de Carvalho, R.R. 1998, AJ, 116, 1591

Poveda, A. 1961, ApJ, 134, 910

Press, W.H., & Schechter, P. 1974, ApJ, 187, 425

Sandage, A., & Visvanathan, N. 1978, ApJ, 225, 742

Scott, S.E., et al. 2002, MNRAS, 331, 817

Sersic, J.L. 1968, Atlas de galaxias australes, Observatorio Astronomico de Cordoba, Argentina

Shankar, F., Salucci, P., Granato, G.L., De Zotti, G., & Danese, L. 2004, MNRAS, 354, 1020

Sheth, R.K., & Tormen, G. 2002, MNRAS, 329, 61

Sheth, R.K., et al. 2003, *ApJ*, 594, 225

Silk, J., & Rees, M.J. 1998, *A&A*, 331, L1

Silva, L., De Zotti, G., Granato, G.L., Maiolino, R., & Danese, L. 2005, *MNRAS*, in press (astro-ph/0412340)

Silva, L., Granato, G.L., Bressan, A., & Danese, L. 1998, *ApJ*, 509, 103

Somerville, R.S., et al. 2004, *ApJ*, 600, 135

Tecza, M., et al. 2004, *ApJ*, 605, 109

Terlevich, A.I., & Forbes, D.A. 2002, *MNRAS*, 330, 547

Trager, S.C., Faber, S.M., Worthey, G., & González, J.J. 2000, *AJ*, 120, 165

Tremaine, S., et al. 2002, *ApJ*, 574, 740

Treu, T., Stiavelli, M., Bertin G., Casertano, C., & Møller, P. 2002, *ApJ*, 564, L13

Trujillo, I., Burkert, A., & Bell, E.F. 2004, *ApJ*, 600, 39

Umemura, M. 2001, *ApJ*, 560, L29

Valluri, M., Ferrarese, L., Merritt, D., & Joseph, C.J. 2005, astro-ph/0502493

van der Marel, R.P. 2003, in Carnegie Observatories Astrophysics Series, Vol. 1: Coevolution of Black Holes and Galaxies, ed. L.C. Ho (Cambridge Univ. Press), in press, (astro-ph/0302101)

van der Wel, A., Franx, M., van Dokkum, P.G., & Rix, H.-W. 2004, *ApJ*, 601, L5

Wechsler, R.H., Bullock, J.S., Primack, J.R., Kravtsov, A.V., & Dekel, A. 2002, *ApJ*, 568, 52

White, S.D.M., & Frenk, C.S. 1991, *ApJ*, 379, 52

Zhao, D.H., Jing, Y.P., Mo, H.J., & Börner, G. 2003a, *ApJ*, 597, L9

Zhao, D.H., Mo, H.J., Jing, Y.P., & Börner, G. 2003b, *MNRAS*, 339, 12